ChemPubSoc Europe

DOI: 10.1002/cmdc.201500385

CHEMMEDCHEM Full Papers

SPECIAL ISSUE

Potent and Selective Inhibitors of *Trypanosoma cruzi* Triosephosphate Isomerase with Concomitant Inhibition of Cruzipain: Inhibition of Parasite Growth through Multitarget Activity

Elena Aguilera,[a] Javier Varela,[a] Estefanía Birriel,[a] Elva Serna,[b] Susana Torres,[b] Gloria Yaluff,[b] Ninfa Vera de Bilbao,[b] Beatriz Aguirre-López,[c] Nallely Cabrera,[c] Selma Díaz Mazariegos,[c] Marieta Tuena de Gómez-Puyou,[c] Armando Gómez-Puyou,[c] Ruy Pérez-Montfort,[c] Lucia Minini,[d] Alicia Merlino,[d] Hugo Cerecetto,[a, e] Mercedes González,[a] and Guzmán Alvarez*[a, f]

Dedicated to the memory of Armando Gómez-Puyou—an exemplary scientist and friend.

Triosephosphate isomerase (TIM) is an essential *Trypanosoma cruzi* enzyme and one of the few validated drug targets for Chagas disease. The known inhibitors of this enzyme behave poorly or have low activity in the parasite. In this work, we used symmetrical diarylideneketones derived from structures with trypanosomicidal activity. We obtained an enzymatic inhibitor with an IC_{50} value of 86 nM without inhibition effects on the mammalian enzyme. These molecules also affected cruzipain, another essential proteolytic enzyme of the parasite. This dual activity is important to avoid resistance problems. The compounds were studied in vitro against the epimastigote form of the parasite, and nonspecific toxicity to mammalian cells was also evaluated. As a proof of concept, three of the best derivatives were also assayed in vivo. Some of these derivatives showed higher in vitro trypanosomicidal activity than the reference drugs and were effective in protecting infected mice. In addition, these molecules could be obtained by a simple and economic green synthetic route, which is an important feature in the research and development of future drugs for neglected diseases.

Introduction

Chagas disease is caused by the parasite *Trypanosoma cruzi*. It remains the major parasitic disease in Latin America, despite recent advances in the control of its vector-borne and transfusion-mediated transmission.[1] Moreover, migration of infected people has spread the disease to non-endemic areas, presenting a new worldwide challenge.[2] The chemotherapy regime employed to control the parasitic infection employs old and nonspecific drugs, such as Nifurtimox and Benznidazole, and requires long-term treatment that can give rise to severe side effects.[3] Although Nifurtimox and Benznidazole are able to eliminate patent parasitemia and decrease serological titers in acute and early chronic infections, they are not active against all *T. cruzi* strains, exhibit low efficiency in long-term chronic infections, and are mutagenic.[4] Unfortunately, due to a perceived deficit in potential revenue, most pharmaceutical companies have neglected this disease despite the urgent need for new drugs.

A variety of molecular targets has been identified for designing new drugs, among which are metabolites formed during sterol biosynthesis, glycolysis, and DNA synthesis.[5,6] An important characteristic of *T. cruzi* is its dependence on glycolysis as an energy source for cellular survival.[7] Thus, enzymes of this

[a] *E. Aguilera, J. Varela, E. Birriel, Dr. H. Cerecetto, Dr. M. González, Dr. G. Alvarez*
Grupo de Química Medicinal, Facultad de Ciencias
Universidad de la República, Iguá 4225, Montevideo, 11600 (Uruguay)

[b] *E. Serna, S. Torres, G. Yaluff, Dr. N. V. de Bilbao*
Departamento de Medicina Tropical
Instituto de Investigaciones en Ciencias de la Salud
Universidad Nacional de Asunción, Asunción, 2511 (Paraguay)

[c] *B. Aguirre-López, N. Cabrera, S. Díaz Mazariegos, Dr. M. T. de Gómez-Puyou, Dr. A. Gómez-Puyou, Dr. R. Pérez-Montfort*
Departamento de Bioquímica y Biología Estructural
Instituto de Fisiología Celular
Universidad Nacional Autónoma de México, México DF, 04510 (México)

[d] *L. Minini, Dr. A. Merlino*
Laboratorio de Química Teórica y Computacional, Facultad de Ciencias
Universidad de la República, Iguá 4225, Montevideo, 11600 (Uruguay)

[e] *Dr. H. Cerecetto*
Área de Radiofarmacia, Centro de Investigaciones Nucleares
Facultad de Ciencias, Universidad de la República
Iguá 4225, Montevideo, 11600 (Uruguay)

[f] *Dr. G. Alvarez*
Laboratorio de Moléculas Bioactivas
Centro Universitario Regional Litoral Norte
Universidad de la República, Rute 3 km 363, Paysandú, 60000 (Uruguay)
E-mail: guzmanalvarezlqo@gmail.com

Supporting information and ORCID(s) from the author(s) for this article are available on the WWW under http://dx.doi.org/10.1002/cmdc.201500385.

This article is part of a Special Issue on Polypharmacology and Multitarget Drugs. To view the complete issue, visit: http://onlinelibrary.wiley.com/doi/10.1002/cmdc.v11.12/issuetoc.

pathway represent excellent targets for research of small molecules that could inhibit them selectively and affect their metabolic function.

In this sense, *T. cruzi* triosephosphate isomerase (*Tc*TIM) has been proposed as a validated target for drug design against this parasite.[8] TIM catalyzes the isomerization of glyceraldehyde-3-phosphate and dihydroxyacetone phosphate in the fifth step of the glycolytic pathway. Structurally, most known TIMs are homodimers, with each monomer consisting of eight parallel β-strands, surrounded by eight α-helices and forming a barrel. An important feature of the TIM active site is the concerted closure of loop 6 and loop 7 on ligand binding, shielding the catalytic site from bulk solvent. The buried active site stabilizes the enediolate intermediate. The catalytic residue Glu167 is at the top of loop 6. On closure of loop 6, the Glu167 carboxylate moiety moves approximately 2 Å towards the substrate. The dynamic properties of the Glu167 side chain in the enzyme–substrate complex are a key feature of the proton shuttling mechanism. Two proton shuttling mechanisms, the classical and the criss-cross mechanism, are responsible for the interconversion of the substrates of this enolizing enzyme. The interface between monomers occupies a significant portion of the molecular surface area of each monomer, approximately 1496 Å^2 for *Tc*TIM.[9] Interestingly, TIM is active only as a dimer; therefore, the use of small molecules to target its interface may potentially induce structural modifications and alter the dimer, leading to enzyme inactivation.[10] TIM from *homo sapiens* (*Hs*TIM) and the *T. cruzi* enzyme have the same catalytic residues. However, the identity of the approximately 32 interfacial residues of *Tc*TIM and *Hs*TIM is 52%, whereas the identity of those residues between *Tc*TIM and TIM from *Trypanosoma brucei* (*Tb*TIM) is approximately 82%.[11] Therefore, it is theoretically possible to find molecules that have high specificity for the interface of the enzymes from these parasites.[11] As part of an ongoing program in the research for molecules that could provide leads in the design of a new drug for the treatment of Chagas disease, in a previous work, we undertook a massive screening for *Tc*TIM inhibitors. Initially, we performed a primary screening of 230 compounds from an in-house chemical library.[12] The IC_{50} and the selectivity for *Tc*TIM were then determined for the best inhibitors, and we found that some of the best inhibitors of *Tc*TIM were symmetric molecules (Figure 1 A).[12]

Also a lot of simple molecules with structural symmetry have shown trypanosomicidal activity, like curcumin derivatives and others with more complex structures.[13–16] In addition, results obtained in a previous study using a phenotypic screening of *T. cruzi* on near 80 new thiazolyl derivatives allowed the identification of a new bioactive structural motif.[17]

In order to obtain derivatives with inhibitory action on *Tc*TIM and with good activity against *T. cruzi*, we selected frameworks from the diarylideneketone and furylthiazolidine systems (Prototype I and Prototype II in Figure 1 B, respectively), and redesigned the synthesis to obtain simpler and symmetrical molecules. In particular, we replaced the diarylidene system (Figure 1 B) with the furylidene motif previously described to have good trypanosomicidal activity.[12,13,16,17]

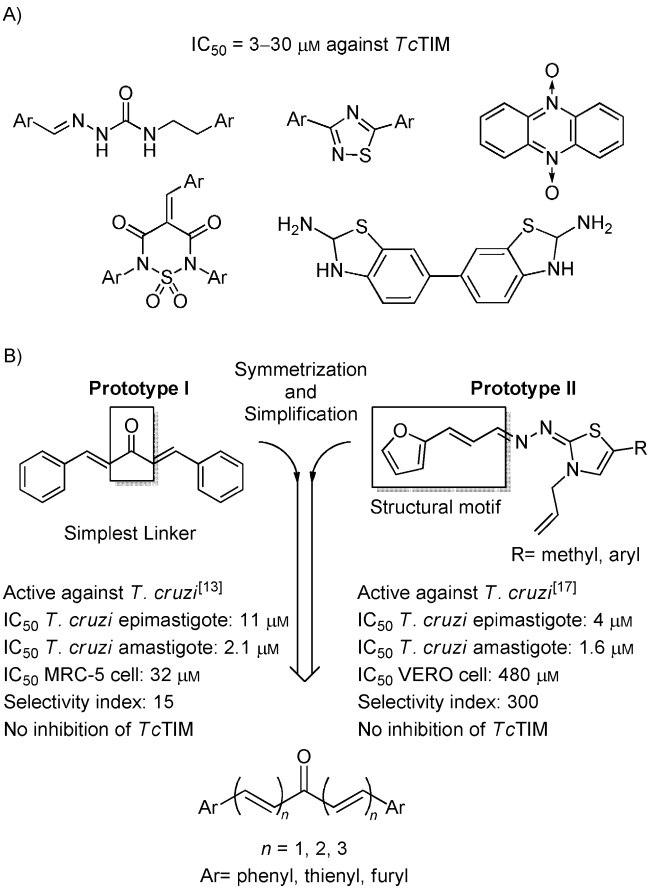

Figure 1. A) Symmetric inhibitors of *Tc*TIM previously reported; Ar denotes an aryl group. B) Trypanosomicidal structures used as basis for designing new and simpler symmetric diarylideneketone from dibenzalketone (Prototype I) and furylthiazolidines (Prototype II) with some of their biological data.[12,13,17]

Results and Discussion

Synthesis of diarylideneketones

The scope of the design of these molecules was the presence of the pharmacophore identified in the previous work: the furylpropenyl fragment.[14] We synthesized 23 derivatives (Tables 1 and 2) with good to excellent yields (60–100%). The synthesis was carried out with environmentally friendly solvents. In most cases, the purification was done by crystallization from ethanol. Consequently, these compounds follow the principles of green chemistry with simple, economical, and environmentally friendly synthesis.[17] For example, the synthesis of one of the most active compounds was performed using furfural, which can be obtained from rice husk (a waste material from the food industry), acetone, ethanol, sodium hydroxide, and water—all reagents being inexpensive and easy to acquire.[18–20]

Anti-*T. cruzi* activity in vitro

The derivatives were initially tested in vitro against the epimastigote form of *T. cruzi*, Tulahuen 2 strain, discrete typing unit (DTU) Tc VI. The compounds were incorporated into the culture

Table 1. Compounds derived from prototype II. Structures of the newly developed compounds, their trypanosomicidal activity against epimastigotes of *Trypanosoma cruzi*, and cytotoxicity against mammalian cells.

Compd	Structure	IC_{50} [μM] *T. cruzi*[a]	IC_{50} [μM] J774.1[b]	SI[c]
Prototype II	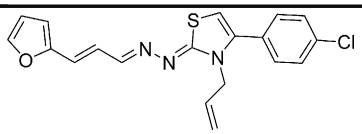	4.2 ± 0.4[d]	120 ± 5[d]	28[d]
1	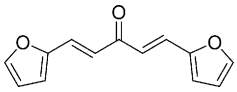	23.9 ± 1.5	115 ± 6	5
2	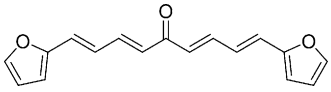	5.0 ± 0.7	60 ± 3	12
3	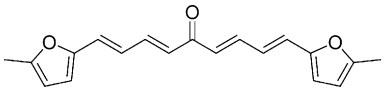	9.4 ± 1.4	ND[e]	–
4	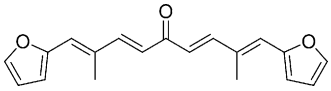	8.2 ± 2.0	33 ± 5	4
5	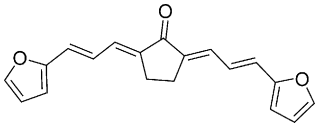	5.4 ± 1.6	19 ± 2	4
6	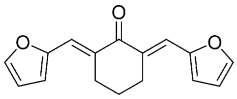	7.3 ± 1.6	115 ± 5	16
7	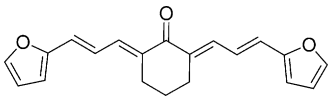	0.6 ± 0.2	10 ± 2	17
8	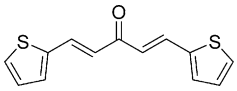	5.0 ± 0.8	38 ± 4	8
9	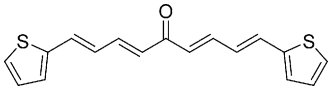	12.6 ± 1.4	188 ± 6	15
10	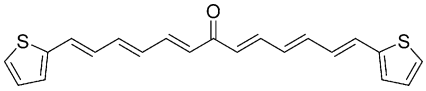	> 25	ND[e]	–
11	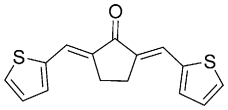	6.5 ± 1.1	ND[e]	–
12	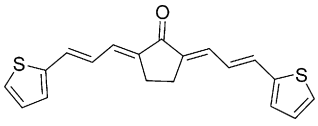	0.04 ± 0.01	15 ± 4	375
13	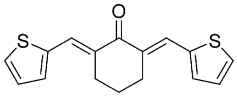	3.6 ± 0.9	73 ± 4	20
14	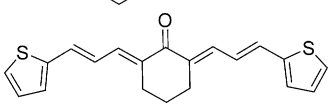	0.6 ± 0.2	20 ± 1	33

milieu at a final concentration of 25 μM, and their ability to inhibit the parasite growth was evaluated and compared to the control (without drug) on day 5. The IC_{50} was determined for the most active derivatives and for Nifurtimox used as the reference drug (Table 1and 2). The 58% of the synthesized molecules displayed good to excellent trypanosomicidal activity ($IC_{50} < 25$ μM). In addition, compounds **7**, **12**, and **14**, with IC_{50} in the submicromolar and nanomolar range, exhibited enhanced trypanosomicidal activity relative to Nifurtimox and their parent compounds Prototype I and Prototype II. We confirmed that the incorporation of a furylacroleine fragment increased the trypanosomicidal activity (comparing the activities of compounds **2** and **1**, and **2** and **15**).

Symmetry played a key role in the anti-*T. cruzi* activity of these molecules (based on the activities of compound **23** and the Prototype I). The number of conjugated double bonds, present between the aryl and carbonyl moieties, caused different effects in the trypanosomicidal activity. For example, for the heteroaryl cyclic ketones, the increase in the number of double bonds increased the bioactivity (as seen for the activities of derivative **6** compared with **7**, derivative **11** compared with **12**, or derivative **13** compared with **14**). With the exception of derivatives **1** and **2**, the contrary occurred in the linear ketones (shown by the activities of derivative **8** compared with **9** and **10**, or Prototype I and **15**). Additionally, the data suggest that the incorporation of an electron donor group (like methyl) to the system decreases trypanosomicidal activity (activities of derivative **2** compared to **3** and **4**). In the case of the cycloheptanones, the compounds without the α,β-ketone system, and the compounds without

Table 1. (Continued)

Compd	Structure	IC_{50} [μM] *T. cruzi*[a]	IC_{50} [μM] J774.1[b]	SI[c]
Nifurtimox	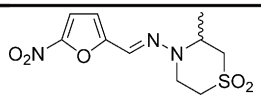	8±1	316±23	40

Compound concentration required to inhibit [a] 50% epimastigote growth of *T. cruzi*, Tulahuen 2 strain or [b] murine macrophages; data represent the mean±SD of two independent experiments performed in triplicate. [c] Selectivity index (SI): IC_{50} against mammalian cells/IC_{50} against *T. cruzi*. [d] Data from Ref. [17]. [e] ND: not determined.

Table 2. Compounds derived from prototype I, the simplest form. Structures of known compounds, their trypanosomicidal activity against epimastigotes of *Trypanosoma cruzi*, and cytotoxicity against mammalian cells.[16]

Compd	Structure	IC_{50} [μM] *T. cruzi*[a]	IC_{50} [μM] J774.1[b]	SI[c]
Prototype I[d]	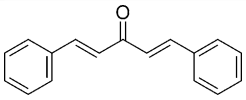	7.2±0.8	22±5	3
15	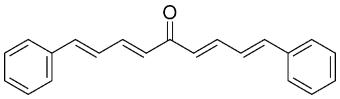	11.0±1.3	50±5	5
16	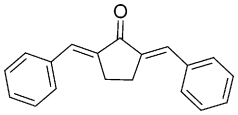	15.9±1.2	ND[e]	–
17	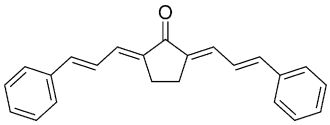	>25	ND[e]	–
18	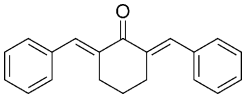	5.1±0.3	115±5	23
19	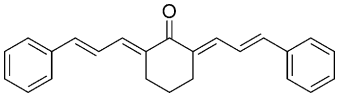	14.2±2.7	168±6	12
20	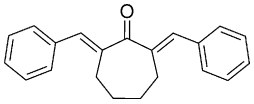	>25	ND[e]	–
21	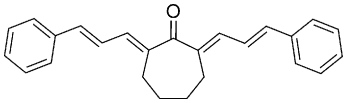	>25	ND[e]	–
22	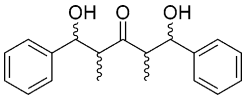	>25	ND[e]	–
23	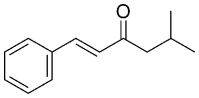	>25	ND[e]	–
Nifurtimox	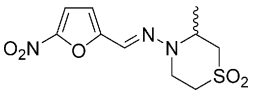	8±1	316±23	40

Compound concentration required to inhibit [a] 50% epimastigote growth of *T. cruzi*, Tulahuen 2 strain or [b] murine macrophages; data represent the mean±SD of two independent experiments performed in triplicate. [c] Selectivity index (SI): IC_{50} against mammalian cells/IC_{50} against *T. cruzi*. [d] Data from Ref. [16]. [e] ND: not determined.

symmetry (compounds **20**–**23**, Table 2), the anti-*T. cruzi* activity decreases dramatically. Furyl-cyclohexanone **7**, thienyl-cyclopentanone **12**, and thienyl-cyclohexanone **14** have trypanosomicidal activity in the submicromolar and nanomolar range. In particular, compound **12** was 200 times more potent than Nifurtimox.

Nonspecific toxicity in mammalian cells in vitro

To explore the selectivity of these new derivatives against *T. cruzi*, we evaluated the nonspecific mammalian cell toxicity in vitro using J774.1 mouse macrophages. The evaluated compounds were selected taking into account their anti-*T. cruzi* activity, and their selectivity indexes were calculated as the ratio between the IC_{50} for mammalian cells and the IC_{50} for *T. cruzi*. The most potent compound against *T. cruzi* (compound **12**) showed an excellent selectivity index (SI), and was 375 times more active against *T. cruzi* than the mammalian cells and near tenfold more selective than the reference drug (Table 1and 2). Comparing the Prototype I with the cyclohexanone **18**, we saw that the flexibility restriction of the molecule by addition of a cycle causes a 7-fold increase in selectivity. Moreover, the extra double bond in derivative **2** relative to **1**, derivative **9** to **8**, derivative **14** to **13**, or derivative **15** to Prototype I, also caused an increase in the selectivity.

Treatment of *T. cruzi*-infected mice

Compounds **2**, **7**, and **12** were evaluated in vivo in a murine model of acute Chagas disease. The chosen compounds for this in vivo assay were the most structurally representative and active molecules of the family of

compounds, with lower nonspecific toxicity and good trypanosomicidal activity. Compound **14** was not tested in vivo because it was a less potent inhibitor of TIM than compound **7** (see below). Benznidazole was used as the reference drug. For optimum oral administration we selected a microemulsion as vehicle which previously demonstrated good bioavailability with compounds like Prototype II.[17] For the experiment, eight male BALB/c mice, infected with CL Brener clone, DTU Tc VI, were treated orally, by intragastric cannula, during 15 days with compounds **2**, **7**, and **12** at 192 μmol kg^{-1} body weight/day (the optimal dose previously established for Prototype II)[17] and compound **7** at 384 μmol kg^{-1} body weight/day in the microemulsion, or Benznidazole at 192 μmol kg^{-1} body weight/day in saline solution. The course of the infection was monitored by counting blood parasites and animal survival, and was followed during 60 days postinfection, in two independent experiments. Derivative **2** led to a significant decrease of the parasitemia (over 50% in the maximum peak of parasitemia and in the second peak, Figure 2) and 83% survival of the treated mice (versus 50% for untreated animals in the same assay). To avoid this fact, a longer duration of treatment could reverse this situation. In other experiments, derivative **7** at the two analyzed doses showed significant decrease of the parasitemia level, but no differences were observed in the double dose (×2) treatment. Derivative **7**, mainly at the lower assayed dose, was able to shift the maximum parasitemia peaks, from day 21 to 28, and day 38 to 45. Additionally, derivative **7** produced a survival of 100% of the animals during the assay. Derivative **12** showed some toxicity achieving significantly reduced parasitemia, although there was a 40% survival of the animals. This goes in contrast to the shown in vitro selectivity index (Table 1). Additionally, derivative **12** was able to abolish the second maximum peak of parasitemia.

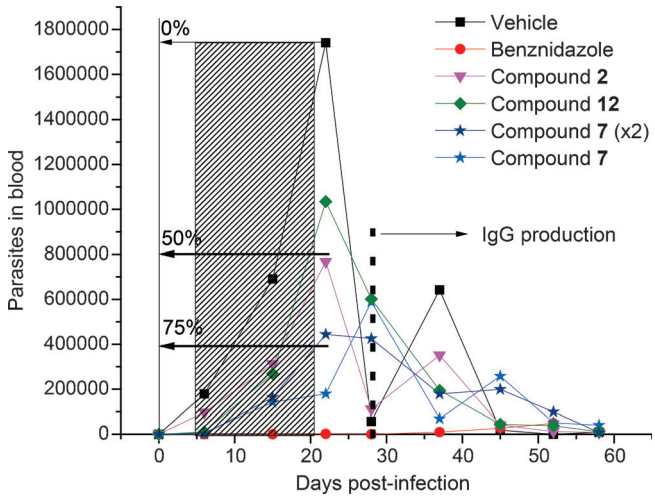

Figure 2. In vivo study of compounds **2**, **7**, and **12** in the acute model of Chagas disease. Curve of parasitemia (parasites per mL of blood) at days postinfection was compared with the control untreated mice (vehicle). The shaded zone shows the treatment period (15 days), and the dashed line marked with IgG shows the start of immune system protection (around 30 days postinfection). Treatments with compound **2** at 192 μmol kg^{-1} body weight/day, compound **7** at 192 or 384 μmol kg^{-1} body weight/day, compound **12** at 192 μmol kg^{-1} body weight/day, and Benznidazole at 192 μmol kg^{-1} body weight/day are shown. Each point represents the average parasitemia of eight mice in each group every seven days. The percentage was calculated from the decrease in the parasitemia peak related to the maximum peak, corresponding to the group of untreated mice. The use of eight mice determines that the results are statistically correct.

Inhibition of triosephosphate isomerase

In order to investigate if these compounds act on *Tc*TIM, we initially tested all of them against the enzyme at a concentration of 25 μM using percentages of inhibition higher than 70% as an arbitrary cut-off point. Some compounds precipitated at 25 μM, leading to variability in the data inhibition at this point. We could not reach 100% inhibition for this reason. Using this cut-off, we detected one new inhibitor (derivative **7**) of *Tc*TIM with better inhibition capacity than the thiadiazolone inhibitor previously described by our group (Table 3).[21,22] Derivative **7** was 40 times more potent than the thiadiazolone and in our knowledge is the best *Tc*TIM inhibitor described until now. Additionally, derivatives **1**, **2**, **4**, **12**, **13**, **14**, and **17** also displayed good IC_{50} but higher than the corresponding values for derivative **7**. It is worth noting that the lack of the extra double bond in compound **1** causes a little decrease in the inhibitory capacity compared with compound **2**. The symmetry of the molecules and the size and the type of the heteroatom present in the aryl ring are important for the inhibition of *Tc*TIM (see molecular docking results in the section below).

To test the selectivity of the inhibition, derivatives **2**, **7**, and **12** were assayed on *Tb*TIM and *Hs*TIM. These compounds were unable to inactivate *Tb*TIM or *Hs*TIM at concentrations higher than 100 μM (see example for **7** in Figure 3). These results confirmed the selectivity and the specificity of these molecules for *Tc*TIM. The destabilization of the dimer was studied using size-exclusion chromatography of *Tc*TIM, in the absence and presence of derivative **7**. We compared the effect of derivative **7** with a monomerization agent like methyl methanethiosulfonate (MMTS).[7] This study showed that the enzyme always elutes as a dimer (Figure S1 in the Supporting Information). These results indicated that the cause of inhibition of *Tc*TIM by derivative **7** does not involve the disruption of the dimer.

Inhibition of cruzipain

When we observed that the activity of the studied compounds in the parasite was not explained only by the TIM inhibition, we decided to explore another target. In order to investigate if the studied compounds were also inhibitors of another molecular target in the parasite, we tested their activity on cruzipain. Cruzipain is a cysteine protease of *T. cruzi* that has been validated as a target because inhibitors of this enzyme affect the evolution of the pathology.[6] We initially tested all derivatives against the enzyme at a concentration of 100 μM using percentages of inhibition higher than 30% as an arbitrary cut-off point. Using this cut-off, we detected two new inhibitors (derivatives **7** and **14**) of cruzipain (Table 4). This enzyme was purified from epimastigotes, and it is important to highlight that the activity in this type of enzyme is more representative than

Table 3. IC_{50} values against *T. cruzi* triosephosphate isomerase (*Tc*TIM) of the best enzymatic inhibitors.

Compd	Structure	IC_{50} [μM][a]
Prototype II	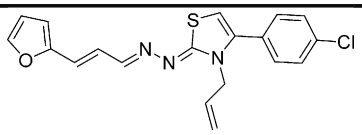	>25
1	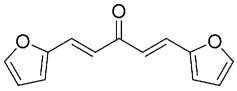	5±1
2	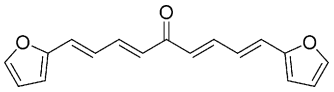	3.0±0.7
4	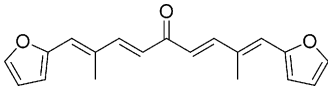	3.3±0.5
7	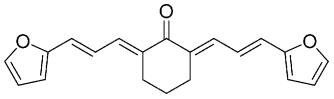	0.086±0.007
12	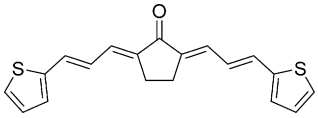	4.7±0.8
13	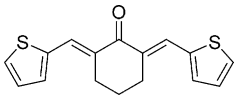	6±1
14	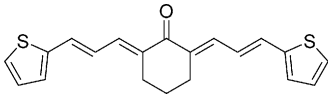	7±1
Prototype I	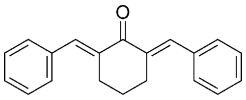	>25
17	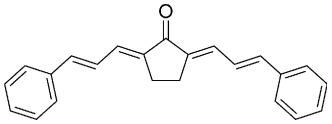	7±1
Thiadiazolone[b]	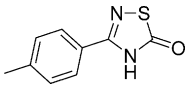	3.5±0.5

[a] IC_{50} values against *Tc*TIM; data represent the mean±SD of two independent experiments performed in triplicate. [b] Inhibitor described previously.[18,19]

the activities in the recombinant version of the enzyme (called cruzain). In the recombinant version one can find inhibitors in the nanomolar range, but in the version purified from epimastigotes (called cruzipain) in the micromolar range.[23,32] We found other derivatives with moderate activity in cruzipain: compounds **2**, **8**, **18**, and **19**. The other tested compounds did not affect the enzyme at a concentration of 100 μM.

We think that the trypanosomicidal activity of the studied compounds could also be explained by affecting other targets like trypanothione reductase,[16] and/or glutatione *S*-tranferase, since we have found inhibition of the last enzyme in other parasites (data not shown).

Molecular docking studies

Molecular docking studies were performed after inhibition experiments to investigate the binding mode of three inhibitors of *Tc*TIM, derivatives **1**, **2**, and **7**, and one derivative with no ability to inhibit *Tc*TIM, derivative **9**. The binding mode of derivative **2** to *Hs*TIM was also analyzed in order to explain its selectivity for *Tc*TIM. The predicted binding modes of derivatives **1**, **2**, **7**, and **9** to *Tc*TIM are shown in Figure 4A–D, and the docking model for derivative **2** with *Hs*TIM is shown in Figure 5.

As illustrated in Figure 4, derivatives **2** (4B) and **7** (4C) bind to the dimer interface. These compounds, having an additional double bond relative to compound **1** (4A), demonstrate the importance of the distance between the two aryl rings as a requirement to bind to the dimer interface. Additionally, the predicted binding mode for derivative **1** (Figure 4A) explains its lower activity, since it binds to a loop at the surface of the enzyme and, thus, can be easily removed from this site due to *Tc*TIM dynamics in solution.[36] Comparing the binding modes of derivative **2** and **9** (Figure 4D), it can be seen that the active compound **2** is stabilized in the binding cleft by strong hydrogen-bond interactions. The furyl oxygen of the inhibitor is hydrogen bonded to the backbone nitrogen of Gly100, and the carbonyl oxygen of the inhibitor interacts with Arg95 side chain (3.0 Å and 2.9 Å, respectively). These interactions were absent in compound **9**. Therefore, besides the conjugate double bonds, the presence of a furyl ring in the molecule is a structural requirement to adequately position the molecule to exert its inhibitory activity against *Tc*TIM. On the other hand, derivative **7**, which inhibits the enzyme in the nanomolar range, is also located in at the interface establishing hydrophobic interactions with Tyr99 and Phe72 of both monomers, and the furyl rings also provide π-cation and π–π-type interactions with residues of Lys110 (monomer A) and Phe72 (monomer B), respectively (Figure 4C). Interestingly, residue Phe72 is located in loop 3, which is involved in maintaining the integrity of the

Table 4. IC_{50} values against cruzipain of the best enzymatic inhibitors of *T. cruzi* triosephosphate isomerase (*Tc*TIM).

Compd	Structure	IC_{50} [μM][a]	Inhibition [%][b]
2	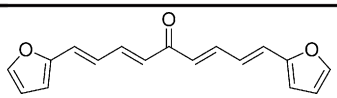	–	48%
7	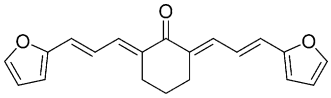	37.0 ± 1.1	–
8	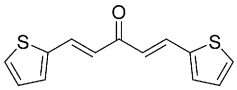	–	49%
12	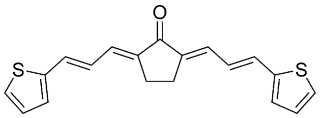	42 ± 2	–
18	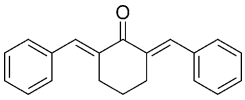	–	38%[c]
19	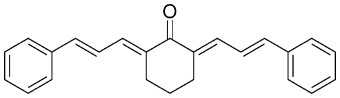	–	40%

[a] IC_{50} values against cruzipain; data represent the mean ± SD of two independent experiments performed in triplicate. [b] Percent inhibition of *Tc*TIM at a compound concentration of 100 μM. [c] According to Ref. [16], at 100 μM, this compound inhibits 31% of the activity of recombinant cruzain.

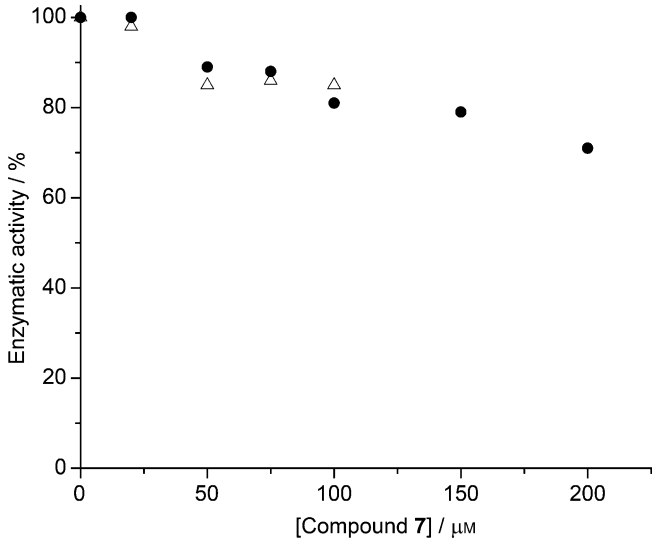

Figure 3. Enzyme inhibition studies. *Hs*TIM (●) and *Tb*TIM (△) activity vs. concentration of compound **7**. Data points represent the mean for triplicates in two independent experiments.

dimer. Comparing derivatives **2** and **7**, one can see that derivative **7** has a restricted movement and a defined orientation because of the chair-like conformation of the cyclohexyl moiety. This orientation increases the π–π interactions. The predicted binding mode of derivative **2** to *Hs*TIM is shown in Figure 5. Clearly, derivative **2** was unable to bind to the dimer interface in *Hs*TIM. Instead, it interacts weakly on the enzyme's surface, which could explain the selectivity of this compound for *Tc*TIM.

Integration of the data

We found three molecules with improved in vitro trypanosomicidal activity in the nanomolar range: compounds **7**, **12**, and **14**. These molecules were more active than the reference drug (Nifurtimox).

Analyzing the whole population of compounds and from the small differences in their structures, it can be said that those containing furyl and thienyl rings are the most active compounds, and the optimal number of conjugated double bonds is four, for the symmetric forms. Also, the movement restriction of the α-carbonyl-carbon improves trypanosomicidal activity. Moreover, this restriction of rotation seems to increase the selectivity. The lack of symmetry leads to loss of trypanosomicidal activity, as seen when comparing compounds **18** with **20** and **23**. Derivatives **2**, **7**, and **12** were able to protect infected animals with *T. cruzi*.

Enzymatic inhibition assays showed that one of the biological targets of derivatives **2** and **7** is *Tc*TIM, an essential enzyme for the metabolism of amastigotes and epimastigotes. A positive qualitative correlation between inhibition of *Tc*TIM and trypanosomicidal activity in vitro was observed. Moreover, compounds **2** and **7** lacked inhibitory activity against *Hs*TIM and *Tb*TIM. Structurally *Tb*TIM is 80% similar to *Tc*TIM, and we demonstrated that it is possible to obtain molecules with specific inhibition of *Tc*TIM besides this apparently small difference between them. The mechanism of inhibition does not involve disruption of the dimer as the other inhibitors previously reported.[24,25] Initially, it was thought that inhibitors targeting the dimer interface caused destabilization and loss of activity. As observed for the MMTS and its analogs, they interact at the interface at Cys15, which is critical for stability.[7,11] Molecular docking studies were consistent with the experimental data, suggest the mechanisms of inhibition, and could explain the selectivity for these novel compounds. Docking results also suggest a possible site of interaction between the inhibitors and *Tc*TIM. It can be seen that the interaction at the interface is located near loop 6 and loop 7, critical loops for the movement of the active site and substrate input. Thus, the inhibitors may stabilize the dimer and prevent the movement necessary for catalysis. Compound **7** was the most potent inhibitor,

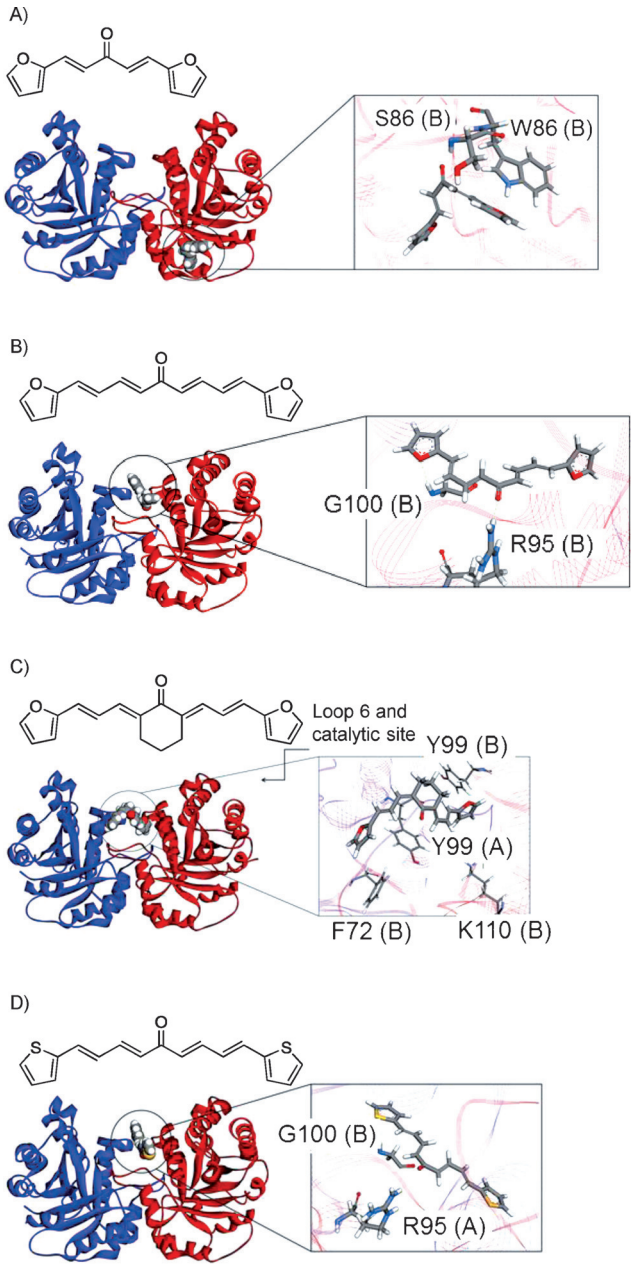

Figure 4. Predicted binding modes. A) Compound **1** did not interact in the interface (too short) and was a moderate inhibitor. B) Compound **2** interacted with the interface and was a good inhibitor. C) Compound **7** interacted with the interface more closely at the critical loop and was the best inhibitor. D) Compound **9** interacted in the interface superficially and was not an inhibitor.

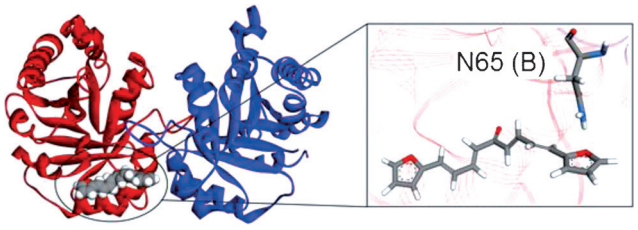

Figure 5. Predicted binding mode of derivative **2** to *Hs*TIM. Derivative **2** did not interact in the interface and did not inhibit the enzyme.

which is 41 times better than the thiadiazolone previously described.[21,22] Additionally, it has in vitro trypanosomicidal activity in the nanomolar range, which is 13 times more active than the reference drug.

Cruzipain inhibition assays showed that another biological target of derivatives **7** and **12** is this essential enzyme. In addition, a positive qualitative correlation between inhibition of cruzipain and trypanosomicidal activity was observed in vitro.

We can hypothesize that the trypanosomicidal activity of derivatives **7** and **12** involve the inhibition of at least two biological targets: *Tc*TIM and cruzipain. Other mechanisms are probably derived from the furylacroleine fragment, a previously described pharmacophore.[17] This fragment could be acting as a substrate for a specific oxidoreductase in the parasite, with the generation of toxic molecules.[26,27] Another target reported for diarylideneketones[13,16] is the thiol metabolism dependent on trypanothione reductase, a flavoenzyme that maintains bis-glutathionylspermidine (trypanothione) and monoglutathionylspermidine in their reduced state. This thiol system replaces the glutathione/glutathione-reductase system (present in mammalian hosts) and is widely accepted as a target for the development of novel therapies to treat trypanosomiasis and leishmaniasis. Finally, another potential target is glutathione *S*-transferase, as part of the same metabolic pathway aforementioned.

Since these compounds are molecules directed to multiple targets, it makes the generation of resistant parasites less likely. In this way, less evolutionary pressure on the parasitic population is generated, thereby lowering the probability of generation of resistance.[28]

Conclusions

A series of highly potent and selective *T. cruzi* growth inhibitors was successfully described. These compounds are structurally different from known compounds, which are less potent and have toxicity liabilities.[12–19] Among them, the most promising compound, derivative **7**, showed efficacy in vivo in the acute model of Chagas disease, with absence of in vivo toxicity and was able to inhibit *Tc*TIM and cruzipain. These results support the progress of this compound as a low-cost multitarget drug candidate.

Experimental Section

General procedure for the synthesis of diarylideneketones 1–21.[29] All characterization data, appearances, yields, spectroscopic data, procedures, and elemental microanalyses are available in the Supporting Information.

In vitro anti-*T. cruzi* test.[17] *T. cruzi* epimastigotes (Tulahuen 2 strain) were grown at 28 °C in brain–heart infusion (BHI)-tryptose milieu supplemented with 5% fetal bovine serum. Cells from a 10-day-old culture (stationary phase) were inoculated into 50 mL of fresh milieu to give an initial concentration of 1×10^6 cells mL^{-1}. Cell growth was followed by measuring the absorbance of the culture at 600 nm every day. Before inoculation, the milieu was supplemented with the indicated quantity (for a first evaluation 25 μM

was used) of the drug from a stock solution in dimethylsulfoxide (DMSO). The final concentration of DMSO in the culture milieu never exceeded 0.4%. Cultures with nontreated epimastigotes and 0.4% DMSO were included as negative controls, while cultures with 8 μM of Nifurtimox were used as positive controls. The percentage of growth inhibition (PGI) was calculated as follows: PGI (%) = $\{1-[(A_p-A_{0p})/(A_c-A_{0c})]\}\times 100$, where $A_p = A_{600}$ of the culture containing the drug at day 5; $A_{0p} = A_{600}$ of the culture containing the drug just after adding the inoculum (day 0); $A_c = A_{600}$ of the culture in the absence of drug (negative control) at day 5; $A_{0c} = A_{600}$ in the absence of the drug at day 0. In order to determine the 50% inhibitory concentration (IC_{50}) values, parasite growth was followed in the absence (negative control) and presence of increasing concentrations of the corresponding drug. At day 5, the absorbance of the culture was measured and related to the control. The IC_{50} value was taken as the concentration of drug needed to decrease the absorbance ratio to 50%. All IC_{50} values in this work were obtained by analysis with the program OriginLab8.5, using sigmoidal regression (PGI vs. logarithm of the compound concentration) and triplicate samples. The positive control PGI was always around 50%.

Nonspecific cytotoxicity assay.[17] J774.1 murine macrophage cells (ATCC, USA) were grown in Dulbecco's Modified Eagle's Medium (DMEM) culture milieu containing 4 mM L-glutamine and supplemented with 10% heat-inactivated fetal calf serum. The cells were seeded in a 96-well plate (5×10^4 cells in 200 μL culture medium) and incubated at 37 °C in a 5% CO_2 atmosphere for 48 h, to allow cell adhesion prior to drug testing. Afterwards, cells were exposed for 48 h to the compounds (12.5–400 μM) or vehicle for control (0.4% DMSO), and additional controls (cells in milieu) were used in each test. Cell viability was then assessed by measuring the mitochondria-dependent reduction of MTT (3-(4,5-dimethylthiazol-2-yl)-2,5-diphenyltetrazolium bromide) to formazan. For this purpose, MTT in sterile PBS (0.2% glucose) pH 7.4 was added to the macrophages to achieve a final concentration of 0.1 mg mL^{-1} and the cells were incubated at 37 °C for 3 h. After removing the milieu, formazan crystals were dissolved in DMSO (180 μL) and MTT buffer (20 μL, 0.1 M glycine, 0.1 M NaCl, 0.5 mM EDTA, pH 10.5), and the absorbance at 560 nm was measured. The IC_{50} was defined as the drug concentration at which 50% of the cells were viable, relative to the control (no drug added), and was determined by analysis using OriginLab8.5 sigmoidal regression (% of viable cells vs. logarithm of the compound concentration) for triplicate samples.

Formulation for in vivo assays.[14,17,30] The lipid-based drug delivery system was prepared using 1.0 g of surfactant (460 mg polyoxyl-40 hydrogenated castor oil, 360 mg of sodium oleate, and 180 mg of soya phosphatidylcholine), 1.0 g of cholesterol, and phosphate buffer enough to make 10 mL of the vehicle. Preparation: each compound was pulverized in a porcelain mortar and mixed with cholesterol, phosphatidylcholine, and polyoxyl-40 hydrogenated castor oil. The mixture was dissolved in $CHCl_3$, and this was evaporated under vacuum to dryness. To ensure complete removal of the $CHCl_3$, a stream of N_2 was passed through the vial for 5 min. In parallel, sodium oleate was dissolved in phosphate buffer and shaken for 12 h at rt in an orbital shaker. This solution was then added to the mix containing the compounds, and the mixture was homogenized and immersed in an ultrasonic bath at full power for 30–60 min until the desired homogeneity and consistency were reached.

In vivo anti-*T. cruzi* activity (acute model).[14,17,31] BALB/c male mice (30 days old, 25–30 g) were infected by intraperitoneal injections of 5×10^3 blood trypomastigotes (CL Brener). One group (eight animals) was used as control (inoculated orally with the vehicle), and two groups of animals were treated with the studied derivatives (eight animals) or Benznidazole (seven animals), respectively. The first parasitemia developed five days postinfection (week 1), and the treatment began seven days later (when 80% of the animals were infected). Compounds were administered orally, using the aforementioned formulation, 0.2 mL at 50 mg kg^{-1} body weight/day, during 15 days (daily, once a day). Parasitemia, in control and treated mice, was determined in tail-vein blood once a week after the first administration during 60 days, and the mortality rate was recorded. The number of parasites (trypomastigotes form) in blood were counted manually in an optical microscope (at 40× magnification). The numbers of parasites in blood were averaged for each group, and the number of parasites in blood vs. time post-infection in days was graphed. The experimental protocols with animals were evaluated and supervised by the local Ethics Committee, and the research adhered to the Principles of Laboratory Animal Care. These recommend five to eight animals per group for a good relation between the number of parasites and errors.

Expression and purification of TIMs. *Tc*TIM, *Tb*TIM, and *Hs*TIM were expressed in *Escherichia coli* and purified as described in the literature.[7–11] After purification, the enzymes were dissolved in 100 mM triethanolamine, 10 mM EDTA ,and 1 mM dithiothreitol (DTT, pH 8) and were precipitated with $(NH_4)_2SO_4$ (75% saturation) for storage at 4 °C. Before use, extensive dialysis against 100 mM triethanolamine, 10 mM EDTA (pH 7.4) was performed. The purity of the protein was analyzed by SDS-PAGE electrophoresis (TIM monomer is 27 kDa). Protein concentration was determined by absorbance readings at 280 nm. The ε ($M^{-1}cm^{-1}$) were 36440 for *Tc*TIM, 33460 for *Tb*TIM, and for *Hs*TIM concentration was determined by Bradford's method, using the Bio-Rad protein assay, with bovine serum albumin as standard.

TIM enzymatic activity and inhibition assays.[14,21,22] Enzymatic activity was determined following the conversion of glyceraldehyde 3-phosphate (GAP) into dihydroxyacetone phosphate. The decrease in absorbance at 340 nm due to oxidation of NADH in a coupled enzyme assay was followed in a multicell Hewlett–Packard spectrophotometer at 25 °C. The reaction mixture (1 mL, pH 7.4) contained 100 mM triethanolamine, 10 mM EDTA, 0.2 mM NADH, 1 mM GAP, and 0.9 units of α-glycerol phosphate dehydrogenase. The reaction was initiated by addition of 1.0 nM of the corresponding TIM or the corresponding TIM preincubated with the studied compounds (from the mixture as described below). In these cases of the inhibition assays, the enzymes at 1.0 μM were preincubated for 2 h at 37 °C with the studied compounds (at different concentrations) in 10% DMSO. The average specific activity of *Tc*TIM with 1 mM GAP as substrate was 3400 μmol (min mg)$^{-1}$ as 100% of activity. The IC_{50} was defined as the drug concentration at which there is only 50% of the initial velocity, relative to the control (no drug added), and was determined by analysis using OriginLab8.5 sigmoidal regression (% of enzymatic activity vs. logarithm of the compound concentration). All assays were done in triplicate, and the average error for each measurement did not exceed 10%.

Cruzipain enzymatic activity and inhibition assays.[23,32] Cruzipain was purified according to the work of Cazzulo et al.[33] Cruzipain (2.5 μM $\varepsilon = 58285\ M^{-1}cm^{-1}$) was incubated in 50 mM acetate buffer pH 5.5 with 50 mM DTT, and 100 μM inhibitor was added, and the solution was shaken for 15 min at 27 °C. The derivatives were added diluted in DMSO, and the controls contained the same sol-

vent concentration. The concentration of DMSO never exceeded 1% in the reaction milieu. E-64 was used as a positive control of inhibition.[32b] Then, the fluorogenic substrate Z-Phe-Arg-AMC (100 μM) was added, and the fluorescence was measured during 10 min at intervals of 3 s (excitation at 350 nm and emission at 460 nm) using a Varioskan Flash Spectrophotometer. From the slope of the negative control, we calculated the total (100%) enzyme activity, while the slopes obtained in the presence of the compounds yielded the percentage of remaining enzyme activity. The percentage of enzyme inhibition was determined as 100% of remaining enzyme activity. The experiments were done in triplicate for two independent experiments.

Dimerization check by size-exclusion fast protein liquid chromatography.[9] *Tc*TIM at a concentration of 8.0 μM in the presence and absence of 10 μM of the studied compound was incubated at 37 °C for 2 h and analyzed immediately in a Superdex 200 10/300 GL (GE Healthcare Life Sciences) column that was previously equilibrated with 100 mM triethanolamine and 10 mM EDTA, pH 7.4. The flow in the column was set to 0.5 mL min^{-1} in an ÄKTA Purifier UV 900 (GE Healthcare Life Sciences). To determine the elution volume of the monomer, *Tc*TIM, at the same concentration of 8.0 μM, was incubated for 2 h at 25 °C with 100 μM MMTS and analyzed immediately in the same column and conditions. The enzymatic activity of each samples were verified before the chromatography.

Ligand–protein molecular docking.[34–40] The geometrical structures of the synthesized compounds were fully optimized in aqueous solution at the PM6 semi-empirical level using IEF-PCM (integral equation formalism polarizable continuum model) with bond atomic radius. Molecular docking calculations were carried out with Autodock 4.2 using the implemented empirical free energy function and the Lamarckian Genetic Algorithm. In order to take into account protein flexibility, the average protein structures for *Tc*TIM[34] and *Hs*TIM[35] (obtained by previous molecular dynamic simulations) were used to perform ligand–protein docking.[36] The AutoDockTools package was employed to generate the docking input files and to analyze the docking results. Gasteiger–Marsilli charges were used for proteins and ligands.[37] Since the location of the compounds in the enzyme was unknown, a grid map with 124×126×126 points and a grid-point spacing of 0.6 Å was applied in order to explore the entire protein surface. The maps were centered on the macromolecule. Each docking consisted of 50 independent runs, with an initial population of 150 individuals, a maximum number of 2.5×10^5 energy evaluations, and a maximum number of 27000 generations. Default values were used for the remaining parameters. Results differing by less than 2.0 Å in root-square deviation were grouped into the same cluster.

Acknowledgements

The authors would like to thank the Comisión Sectorial de Investigación Científica (CSIC) of the Universidad de la República (UdelaR), Montevideo, Uruguay (CSIC–N° 661) for financial support. E. A. thanks the Agencia Nacional de Investigación e Innovación (ANII), Uruguay and the CSIC for her scholarships. This work was also supported by grants from the Consejo Nacional de Ciencia y Tecnología (CONACyT), México (167823 to R. P.-M.) and the Dirección General de Asuntos del Personal Académico (DGAPA–UNAM), México (IN221812 to RP-M).

Keywords: Chagas disease · cruzipain · enzyme inhibitors · multitarget drugs · triosephosphate isomerase · *Trypanosoma cruzi*

[1] C. J. Schofield, J. Jannin, R. Salvatella, *Trends Parasitol.* **2006**, *22*, 583–588.
[2] L. Kapelusznik, D. Varela, S. P. Montgomery, A. N. Shah, F. J. Steurer, D. Rubinstein, S. H. Factor, *Clin. Infect. Dis.* **2013**, *57*, e7.
[3] J. R. Coura, J. Borges-Pereira, *Rev. Soc. Bras. Med. Trop.* **2012**, *45*, 286–296.
[4] M. Cabrera, M. L. Lavaggi, P. Hernández, A. Merlino, M. González, H. Cerecetto, *Toxicol. Lett.* **2009**, *190*, 140–149.
[5] D. Smirlis, M. B. Soares, *Subcell. Biochem.* **2014**, *74*, 43–76.
[6] A. Merlino, M. González, H. Cerecetto, *Curr. Enzyme Inhib.* **2010**, *6*, 195–210.
[7] A. Gómez-Puyou, E. Saavedra-Lira, I. Becker, R. A. Zubillaga, A. Rojo-Domínguez, R. Pérez-Montfort, *Chem. Biol.* **1995**, *2*, 847–855.
[8] A. A. Cortés-Figueroa, A. Pérez-Torres, A. Salaiza, N. Cabrera, N. Escalona-Montaño, A. Rondán, A. Aguirre-García, M. Gómez-Puyou, A. Pérez-Montfort, R. Becker, *Parasitol. Res.* **2008**, *102*, 635–643.
[9] E. Maldonado, M. Soriano-García, A. Moreno, R. Perez-Montfort, *J. Mol. Biol.* **1998**, *283*, 193–203.
[10] V. Olivares-Illana, A. Rodríguez-Romero, I. Becker, M. Berzunza, A. Gómez-Puyou, *PLoS Neglected Trop. Dis.* **2007**, *1*, e1.
[11] V. Olivares-Illana, R. Pérez-Montfort, F. López-Calahorra, M. Costas, A. Rodríguez-Romero, M. Tuena de Gómez-Puyou, A. Gómez Puyou, *Biochemistry* **2006**, *45*, 2556–2560.
[12] G. Álvarez, B. Aguirre-López, J. Varela, M. Cabrera, A. Merlino, G. V. López, M. L. Lavaggi, W. Porcal, R. Di Maio, M. González, H. Cerecetto, N. Cabrera, R. Pérez-Montfort, M. Tuena de Gómez-Puyou, A. Gómez-Puyou, *Eur. J. Med. Chem.* **2010**, *45*, 5767–5772.
[13] E. Davioud-Charvet, I. N. Wenzel, T. J. J. Müller, G. Hanquet, D. A. Lanfranchi, F. Leroux, T. Gendron, (Centre National De La Recherche Scientifique, Paris, France), , **2011**, WO2011/033115 A2.
[14] G. Álvarez, J. Martínez, J. Varela, E. Birriel, E. Cruces, M. Gabay, S. M. Leal, P. Escobar, B. Aguirre-López, N. Cabrera, M. Tuena de Gómez-Puyou, A. Gómez-Puyou, R. Pérez-Montfort, G. Yaluff, S. Torres, E. Serna, N. Vera de Bilbao, M. González, H. Cerecetto, *Eur. J. Med. Chem.* **2015**, *100*, 246–256.
[15] a) T. L. Deepika, K. Kannabiran, V. G. Khanna, G. Rajakumar, A. A. Rahuman, *Parasitol. Res.* **2012**, *111*, 1151–1163; b) D. Saleheen, M. M. Yasinzai, *Biol. Pharm. Bull.* **2002**, *25*, 386–389.
[16] S. F. Braga, E. V. P. Alves, S. R. Ferreira, J. R. B. Fradico, P. S. Lage, M. C. Duarte, T. G. Ribeiro, P. A. S. Júnior, A. J. Romanha, M. L. Tonini, M. Steindel, E. F. Coelho, R. B. de Oliveira, *Eur. J. Med. Chem.* **2014**, *71*, 282–289.
[17] G. Álvarez, J. Varela, P. Márquez, M. Gabay, C. E. Arias Rivas, K. Cuchilla, G. A. Echeverría, O. E. Piro, M. Chorilli, S. M. Leal, P. Escobar, E. Serna, S. Torres, G. Yaluff, N. I. Vera de Bilbao, M. González, H. Cerecetto, *J. Med. Chem.* **2014**, *57*, 3984–3999.
[18] P. T. Anastas, J. C. Warner, *Green Chemistry: Theory and Practice*, Oxford University Press, New York, **1998**, 30.
[19] J. A. Dumesic, Y. Roman-Leshkov, **2007**, (Wisconsin Alumini Research Foundation, Madison, USA), EP2164928 A1.
[20] H. I. El-Subbagh, S. M. Abu-Zaid, M. Mahran, F. A. Badria, A. M. Al-Obaid, *J. Med. Chem.* **2000**, *43*, 2915–2921.
[21] G. Alvarez, B. Aguirre-López, N. Cabrera, E. B. Marins, L. Tinoco, C. I. Batthyány, M. Tuena de Gómez-Puyou, A. Gómez-Puyou, R. Pérez-Montfort, H. Cerecetto, M. González, *J. Enzyme Inhib. Med. Chem.* **2013**, *28*, 981–989.
[22] G. Alvarez, J. Martínez, B. Aguirre-López, N. Cabrera, L. Pérez-Díaz, M. Tuena de Gómez-Puyou, A. Gómez-Puyou, R. Pérez-Montfort, B. Garat, A. Merlino, M. González, H. Cerecetto, *J. Enzyme Inhib. Med. Chem.* **2014**, *29*, 198–204.
[23] a) A. Merlino, D. Benitez, S. Chavez, J. Da Cunha, P. Hernández, L. Tinoco, M. González, *MedChemComm* **2010**, *1*, 216; c) A. Merlino, D. Benitez, N. Campillo, J. Páez, L. Tinoco, M. González, H. Cerecetto, *MedChemComm* **2012**, *3*, 90–101; b) D. M. E. Caputto, L. E. Fabian, D. Benítez, A. Merlino, N. Ríos, H. Cerecetto, G. Y. Moltrasio, A. G. Moglioni, M. González, L. M. Finkielsztein, *Bioorg. Med. Chem.* **2011**, *19*, 6818–6826.

[24] A. K. Yadav, M. Kumar, M. Verma, M. Kumar, M. Kumar, *Basic Res. J. Med. Clin. Sci.* **2014**, *3*, 62 – 66.
[25] Z. Kurkcuoglu, D. Findik, E. D. Akten, P. Doruker, *Biophys. J.* **2015**, *109*, 1169 – 1178.
[26] H. S. Toogood, N. S. Scrutton, *ChemCatChem* **2010**, *2*, 892 – 914.
[27] A. Trochine, G. Álvarez, S. Corre, P. Faral-Tello, R. Durán, C. I. Batthyany, H. Cerecetto, M. González, C. Robello, *Exp. Parasitol.* **2014**, *140*, 33 – 38.
[28] J. J. Lu, Y. T. Wang, *PLoS One* **2012**, *7*, e40262.
[29] a) J. R. Dimmock, G. Y. Kao, *J. Pharm. Sci.* **1994**, *83*, 852 – 858; b) J. S. Yadav, J. Sarma, *Synth. Commun.* **2002**, *32*, 893 – 896; c) A. Barakat, H. K. Fun, *Molecules* **2015**, *20*, 13240 – 13263; d) I. Huber, I. Zupkó, I. Kovács, P. Perjési, *Monatsh. Chem.* **2015**, *146*, 973 – 981.
[30] T. P. Formariz, LA. Chiavacci, M. V. Scarpa, A. A. Silva-Júnior, E. S. Egito, C. H. Terrugi, C. M. Franzini, V. H. Sarmento, A. G. Oliveira, *Colloids Surf. B* **2010**, *77*, 47 – 53.
[31] D. B. Morton, P. H. Griffiths, *Vet. Rec.* **1985**, *116*, 431 – 436.
[32] a) M. Couto, C. Sánchez, B. Dávila, V. Machín, J. Varela, G. Álvarez, M. Cabrera, L. Celano, B. Aguirre-López, N. Cabrera, M. Tuena de Gómez-Puyou, A. Gómez-Puyou, R. Pérez-Montfort, H. Cerecetto, M. González, *Molecules* **2015**, *20*, 14595 – 14610; b) N. Fujii, J. P. Mallari, E. J. Hansell, Z. Mackey, P. Doyle, Y. Zhou, J. H. McKerrow, K. Guy, *Bioorg. Med. Chem. Lett.* **2005**, *15*, 121 – 123.
[33] C. Labriola, M. Sousa, J. J. Cazzulo, *Biol. Res.* **1993**, *26*, 101 – 107.
[34] P. Ostoa-Saloma, G. Garza-Ramos, R. Pérez-Montfort, *Eur. J. Biochem.* **1997**, *244*, 700 – 705.
[35] V. Mainfroid, S. C. Mande, K. Goraj, *Biochemistry* **1996**, *35*, 4110 – 4117.
[36] L. Minini, L. G. Álvarez, G. M. González, H. Cerecetto, A. Merlino, *J. Mol. Graphics Modell.* **2015**, *58*, 40 – 49.
[37] T. V. Borchert, R. K. Wierenga, *Structure* **1993**, *1*, 205 – 213.
[38] J. Gasteiger, M. Marsili, *Tetrahedron* **1980**, *36*, 3219 – 3228.
[39] G. M. Morris, R. K. Belew, D. S. Goodsell, A. J. Olson, *J. Comput. Chem.* **2009**, *30*, 2785 – 2791.
[40] X. G. Gao, E. Maldonado, A. Gómez-Puyou, A. Rodríguez-Romero, *Proc. Natl. Acad. Sci. USA* **1999**, *96*, 10062 – 10067.

Received: August 31, 2015
Published online on October 23, 2015